ADVANCED FUNCTIONAL MATERIALS
www.afm-journal.de

Linking Group Influences Charge Separation and Recombination in All-Conjugated Block Copolymer Photovoltaics

*Jorge W. Mok, Yen-Hao Lin, Kevin G. Yager, Aditya D. Mohite, Wanyi Nie, Seth B. Darling, Youngmin Lee, Enrique Gomez, David Gosztola, Richard D. Schaller, and Rafael Verduzco**

All-conjugated block copolymers bring together hole- and electron-conductive polymers and can be used as the active layer of solution-processed photovoltaic devices, but it remains unclear how molecular structure, morphology, and electronic properties influence performance. Here, the role of the chemical linker is investigated through analysis of two donor–linker–acceptor block copolymers that differ in the chemistry of the linking group. Device studies show that power conversion efficiencies differ by a factor of 40 between the two polymers, and ultrafast transient absorption measurements reveal charge separation only in block copolymers that contain a wide bandgap monomer at the donor–acceptor interface. Optical measurements reveal the formation of a low-energy excited state when donor and acceptor blocks are directly linked without this wide bandgap monomer. For both samples studied, it is found that the rate of charge recombination in these systems is faster than in polymer–polymer and polymer–fullerene blends. This work demonstrates that the linking group chemistry influences charge separation in all-conjugated block copolymer systems, and further improvement of photovoltaic performance may be possible through optimization of the linking group. These results also suggest that all-conjugated block copolymers can be used as model systems for the donor–acceptor interface in bulk heterojunction blends.

1. Introduction

All-conjugated block copolymers are promising materials for use in solution processed organic photovoltaics (OPVs).[1–3] These materials can produce OPV active layers with well-defined donor and acceptor domains through block copolymer self-assembly, which is of interest for the development of high-efficiency OPVs and for achieving a better fundamental understanding of the photoconversion process in organic donor–acceptor heterojunctions. Recent work reported all-conjugated block copolymers with 3% power conversion efficiencies, demonstrating their feasibility and potential for use in OPVs.[4] However, a clear understanding of the molecular characteristics that govern their performance in photovoltaic devices is lacking.

The linking group between polymer blocks serves to covalently link donor and acceptor polymer blocks but may

J. W. Mok, Dr. Y.-H. Lin, Prof. R. Verduzco
Department of Chemical and Biomolecular Engineering
Rice University
Houston, TX 77005, USA
E-mail: rafaelv@rice.edu
Dr. K. G. Yager
Center for Functional Nanomaterials
Brookhaven National Laboratory
Upton, NY 11973, USA
Dr. A. D. Mohite, Dr. W. Nie
Center for Integrated Nanotechnologies Materials Physics and Applications Division
Los Alamos National Laboratory
Los Alamos, NM 87545, USA
Dr. S. B. Darling, Dr. D. Gosztola, Prof. R. D. Schaller
Center for Nanoscale Materials
Argonne National Laboratory
Argonne, IL 60439, USA
Dr. S. B. Darling
Institute for Molecular Engineering
The University of Chicago
Chicago, IL 60637, USA
Dr. Y. Lee, Prof. E. Gomez
Department of Chemical Engineering
The Pennsylvania State University
University Park, PA 16802, USA
Prof. R. D. Schaller
Department of Chemistry
Northwestern University
Evanston, IL 60208, USA
Prof. R. Verduzco
Department of Materials Science and NanoEngineering
Rice University
Houston, TX 77005, USA

DOI: 10.1002/adfm.201502623

also influence electronic properties, including charge separation and recombination processes at the donor–acceptor interface. While a number of studies have focused on morphology and self-assembly of all-conjugated block copolymer systems, none have analyzed the potential impact of the linking group on charge separation and electronic properties of the donor–acceptor interface.[1–3] In the first example of an all-conjugated block copolymer OPV, Sun et al. incorporated an aliphatic spacer between donor and acceptor polymers to electronically decouple donor and acceptor blocks and reduce the probability for charge recombination.[5] Similarly, in small-molecule donor–acceptor dyads, a spacer between donor and acceptor units has been shown to be necessary for charge separation of photoexcited states.[6] Guo et al. reported all-conjugated block copolymers with a fully conjugated linking group that exhibited the highest performance reported to date in all-conjugated block copolymer systems.[4] Efficient photovoltaic devices are thus possible in fully conjugated donor–acceptor systems, but the optimal structure of the linking group is still unknown. Hinkens et al. studied a systematic series of model donor–acceptor systems and found decreasing electronic coupling with increasing separation between donor and acceptor, suggesting that a spacer may be beneficial for reducing the probability for charge recombination.[7] Johnson et al. reported a model system comprised of a donor polymer terminated by a push–pull monomer. They demonstrated that the orientation of the push–pull monomer was important to the formation of interfacial charge transfer states, leading them to hypothesize that low-energy charge transfer states in fully conjugated block copolymers can impede charge generation, depending on the chemistry of the linker.[8]

Here, we study the role of the linking group between polymer donor and acceptor blocks in fully conjugated block copolymer systems. A combination of OPV device studies, grazing incidence X-ray analysis, and transient absorption spectroscopy was used to understand the potential role of the linking group on photovoltaic performance, optoelectronic properties, and charge separation and recombination. Our results show a clear effect of the linking group on photovoltaic device performance. We find that the linking group influences the characteristics of photoexcited states and the formation of free charges. Our results further show that charge recombination is ultrafast even in high-performance block copowlymer OPVs, suggesting significant room for improvement of photovoltaic performance through further engineering of the linking group chemistry.

2. Results and Discussion

Two all-conjugated block copolymers were prepared for this study, both with poly(3-hexyl thiophene) (P3HT) as the donor block and poly((9,9-dioctylfluorene)-2,7-diyl-alt-[4,7-bis(thiophen-5-yl)-2,1,3-benzothiadiazole]-2,2-diyl) (PTBTF) as the acceptor block (see **Figure 1**). Both block copolymers were synthesized using a two-step synthesis approach involving Grignard metathesis polymerization for the preparation of P3HT followed by a Suzuki or Stille polycondensation reaction for the preparation of the PTBTF block.[4] This synthesis strategy (see Scheme S1 in the Supporting Information) produces block

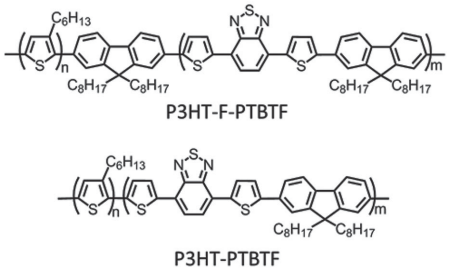

Figure 1. Structure of all-conjugated block copolymers used for this study. The primary difference in the two conjugated block copolymers is the chemistry of the conjugated linking group. Details on the synthesis and characterization of these block copolymers are provided in the Supporting Information.

copolymers with nearly identical constituent blocks but with different monomeric units at the junction between donor and acceptor polymer blocks. Full synthetic details along with ^{1}H nuclear magnetic resonance (NMR) and gel-permeation chromatography (GPC) analysis of the final block copolymers are provided in Figures S1–S3 in the Supporting Information. In the case of P3HT-F-PTBTF, a derivatized fluorene (F unit) resides at the block junction, while for P3HT-PTBTF, the TBT repeat unit forms the block junction. Fluorene is a wide-bandgap monomer, and, qualitatively, serves to electronically decouple P3HT and PTBTF.[8] P3HT-PTBTF does not contain an F unit at the donor–acceptor junction and we would expect greater electronic intermixing at the donor–acceptor interface. The molecular weights, polydispersities, and compositions of the block copolymers are similar, M_n = 26 kDa (PDI = 1.57) for P3HT-F-PTBTF and 20 kDa for P3HT-PTBTF (PDI = 1.37). The P3HT content is 75 wt% for P3HT-F-PTBTF (M_w = 19.4 kDa for the P3HT block) and 70% for P3HT-PTBTF (M_w = 14 kDa for the P3HT block). We also expect roughly 10 wt% homopolymer impurities in both samples.[4]

We investigated the photovoltaic properties of all-conjugated block copolymers in solar cell structures of ITO/PEDOT:PSS/block copolymer/Al. The active layers comprised of pure block copolymers, which were spin cast from either chloroform or a mixture of chloroform and chloronaphthalene (95:5 v/v) at 5.0 mg mL^{-1} concentration, and further annealed at 165 °C for 15 min. Both materials behaved identically in terms of solubility and casting, yielding a film thickness of 70 nm. Current–voltage (J–V) curves of the OPV solar cells illuminated at air mass (AM) 1.5 at 100 mW cm^{-2} are shown in **Figure 2**, and device characteristics are summarized in **Table 1**. The overall power conversion efficiency is roughly 40 times greater for P3HT-F-PTBTF devices compared with devices made from P3HT-PTBTF. The short-circuit current density (J_{SC}) is an order of magnitude larger for P3HT-F-PTBTF block copolymers, and the fill factor (FF) and open-circuit voltage (V_{OC}) are greater for P3HT-F-PTBTF OPV devices. Given the similarities in the composition and structure of the two block copolymers, the large difference in the photovoltaic performance of the materials is surprising.

A number of factors can contribute to power conversion efficiencies, including absorbance, composition, processing history, active layer morphology, charge mobilities, and donor–acceptor interface properties.[2–6] We can exclude composition

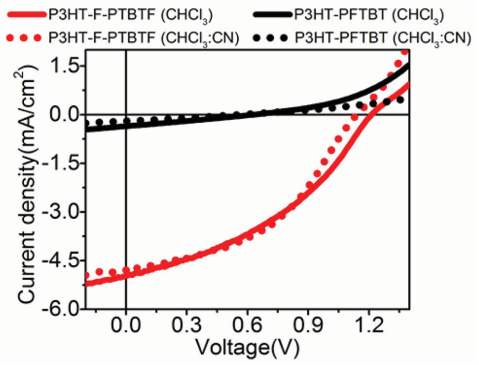

Figure 2. *J–V* curves for block copolymer photovoltaic devices with active layers comprised of P3HT-F-PTBTF (red) or P3HT-PTBTF (black) illuminated at AM 1.5 and 100 mW cm^{-2}.

and processing history as predominant factors since both systems contain the same polymeric donor and acceptor blocks with similar compositions, and the devices were processed using the same procedures. Both samples were purified in a Soxhlet extractor, which removes trace catalyst that may have a detrimental effect on performance.[9] Dark current curves for both devices are shown in Figure S4 in the Supporting Information and indicate a low level of metallic impurities for both samples. Both samples contain homopolymer impurities, and the composition of homopolymer impurities is identical in both samples. Homopolymers are not expected to have strong negative consequences on photovoltaic performance based on prior studies of similar polymer blend devices reported by our group[4] and others.[10–12] We investigated active layer morphology, optical properties, and the lifetimes of charge-separated states as potential factors that might account for such large differences in the photovoltaic performance of the block copolymers studied.

The morphology and crystallinity of the block copolymer films were analyzed by differential scanning calorimetry (DSC) measurements (Figure S5 in the Supporting Information) and grazing incidence X-ray scattering (GIXS) (**Figure 3**). DSC measurements reveal P3HT crystallinity in both samples, with crystal melting temperatures of approximately 220 and 215 °C for P3HT-F-PTBTF and P3HT-PTBTF, respectively. The difference in crystal melting temperatures is attributed to a slightly higher P3HT content in P3HT-F-PTBTF. GIXS measurements provide information on the orientation of crystallites in the block copolymer films, in particular the orientation of the face-to-face π–π stacking of P3HT crystallites. Solution-processed P3HT films and P3HT/PCBM blends typically exhibit an in-plane π–π stacking direction.[13,14] An interesting feature of this block copolymer system is the out-of-plane π–π stacking direction in solution-processed OPV devices. This feature improves charge transport to electrodes.[4,15] As shown in Figure 3, both block copolymer films exhibited peaks characteristic of 2D P3HT crystals with π–π stacking in the out-of-plane direction. The (010) peak corresponds to the π–π stacking direction in P3HT and is strongly oriented out-of-plane (q_z) in both films, indicating that the aromatic stacking is along the film normal. The (100), (200), and (300) peaks correspond to stacking through alkyl side-chains;[16] these peaks exhibited a bimodal orientation distribution, with in-plane (q_x) and out-of-plane (q_z) components. Although these two components appear to have roughly equal scattering intensity, the in-plane peak represents a much larger amount of material since the Ewald sphere intersects only a small piece of a large in-plane scattering ring.[17,18] The orientation distribution of these scattering arcs, taken together, are consistent with a strongly out-of-plane orientation of the π–π stacking direction for both samples processed under conditions identical to those used for devices. Moreover, the orientation distributions appear to be identical for the two materials, and the similar peak widths observed in the GIXS patterns suggest that the crystalline domain sizes are also similar. Grazing incidence small-angle X-ray data is provided in Figure S6 in the Supporting Information and shows no characteristic features for either film;[19] i.e., there is no evidence for differences in the nanoscale morphology. We also provide transmission electron microscopy and atomic force microscopy analysis of both films in Figure S7 in the Supporting Information. Based on these results, we concluded that crystallinity or film morphology does not account for the difference in photovoltaic performance observed for devices made from the two block copolymer samples.

Next, we compared the optical properties of both block copolymers and P3HT and PTBTF homopolymers. P3HT-PFTBT and P3HT-F-PTBTF block copolymers (**Figure 4**a) show almost identical absorption spectra, as expected based on the similar molecular weights and composition of both samples. The absorbance spectra for the block copolymers is roughly the composition-weighted sum of that for each homopolymer block, as has been reported for other all-conjugated block copolymer systems.[13,20] The steady-state photoluminescence (PL) of block copolymers and P3HT and PTBTF homopolymers are also shown in Figures 4a,b. P3HT-F-PTBTF exhibited a PL spectrum matching that of a blend of P3HT and PTBTF homopolymers, and the PL in P3HT-F-PTBTF was significantly quenched relative to P3HT/PTBTF polymer blend films (see Figure S8 in the Supporting Information). This suggests enhanced energy and/or charge transfer in the P3HT-F-PTBTF films. By comparison, P3HT-PTBTF exhibited an excitation spectrum that is redshifted relative to P3HT-F-PTBTF and P3HT/PTBTF blends. The P3HT-PTBTF block copolymer film also exhibited stronger PL com-

Table 1. Device characteristics of block copolymer OPVs, averaged over six devices.

Active layer	PCE [%]	J_{SC} [mA cm^{-2}]	V_{OC}	FF
P3HT-F-PTBTF($CHCl_3$)	2.01 ± 0.27	4.69 ± 0.25	1.15 ± 0.06	0.378 ± 0.01
P3HT-F-PTBTF($CHCl_3$:CN)	2.24 ± 0.17	4.73 ± 0.17	1.11 ± 0.05	0.424 ± 0.01
P3HT-PTBTF($CHCl_3$)	0.052 ± 0.01	0.355 ± 0.021	0.58 ± 0.05	0.267 ± 0.01
P3HT-PTBTF($CHCl_3$:CN)	0.021 ± 0.01	0.195 ± 0.014	0.39 ± 0.15	0.278 ± 0.02

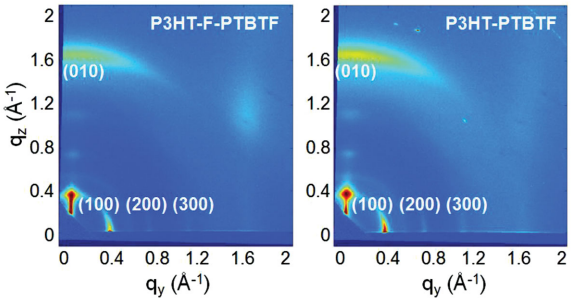

Figure 3. Grazing incidence wide-angle X-ray data from left) P3HT-F-PTBTF and right) P3HT-PTBTF films.

pared with either P3HT-F-PTBTF or a P3HT/PTBTF blend film, as shown in Figure S8 in the Supporting Information.

The redshift in the PL spectra indicates the formation of a unique excited state in P3HT-PFTBT. This excited state is likely formed at the P3HT-TBT junction since this is the only difference between the molecular structures of both samples. This redshift in the PL spectra was also observed in model systems studied by Johnson et al. in which a P3HT oligomer (18 repeat units) was terminated by a single TBTF monomer.[8] We therefore attributed the redshift in the PL of P3HT-PTBTF to the formation of a charge transfer state at the P3HT-TBT junction.

While a clear difference in the PL is observed for these two block copolymers in bulk films, the solution PL for both block copolymers appears virtually identical, as shown in the Figure 4c. The PL of P3HT-PTBTF is not redshifted in solution and matches that of P3HT-F-PTBTF and of homopolymer blends. This suggests that the interfacial excited state responsible for the redshift in the PL spectra of P3HT-PTBTF only forms in bulk films, not in solutions where the polymer chains are disordered.

To gain direct information on the formation and recombination of charge-separated states, ultrafast transient absorption (TA) measurements were carried out on homopolymer and block copolymer films. Analysis of TA signals can provide evidence for the generation of charge-separated states and an estimate of their lifetimes. Prior TA studies have demonstrated that charge-separated states (polarons) in regioregular P3HT exhibit a strong absorption band in the near-IR range (λ = 650–1200 nm).[13,17–20] Thus, populations and lifetimes of charge-separated states in P3HT can be determined through analysis of the photoinduced absorption signal (PIA) at wavelengths of 650–1200 nm.

TA measurements over timescales of 0.1–1000 ps were carried out on P3HT and PTBTF homopolymer films and P3HT-F-PTBTF and P3HT-PTBTF block copolymer films (see **Figure 5**). P3HT and PTBTF homopolymer films exhibit primarily positive differential transmission, reflective of ground-state bleach in the pristine films. In contrast to the homopolymer systems, P3HT-F-PTBTF exhibits a broad PIA from 650–800 nm from 0.1–1000 ps. The observed PIA signal exhibits features almost identical to those of similar polymer photovoltaic blends, such as P3HT and PFTBT, and other P3HT bulk heterojunction OPV systems.[21–26] This PIA is indicative of the creation of charge-separated states in P3HT-F-PTBTF.

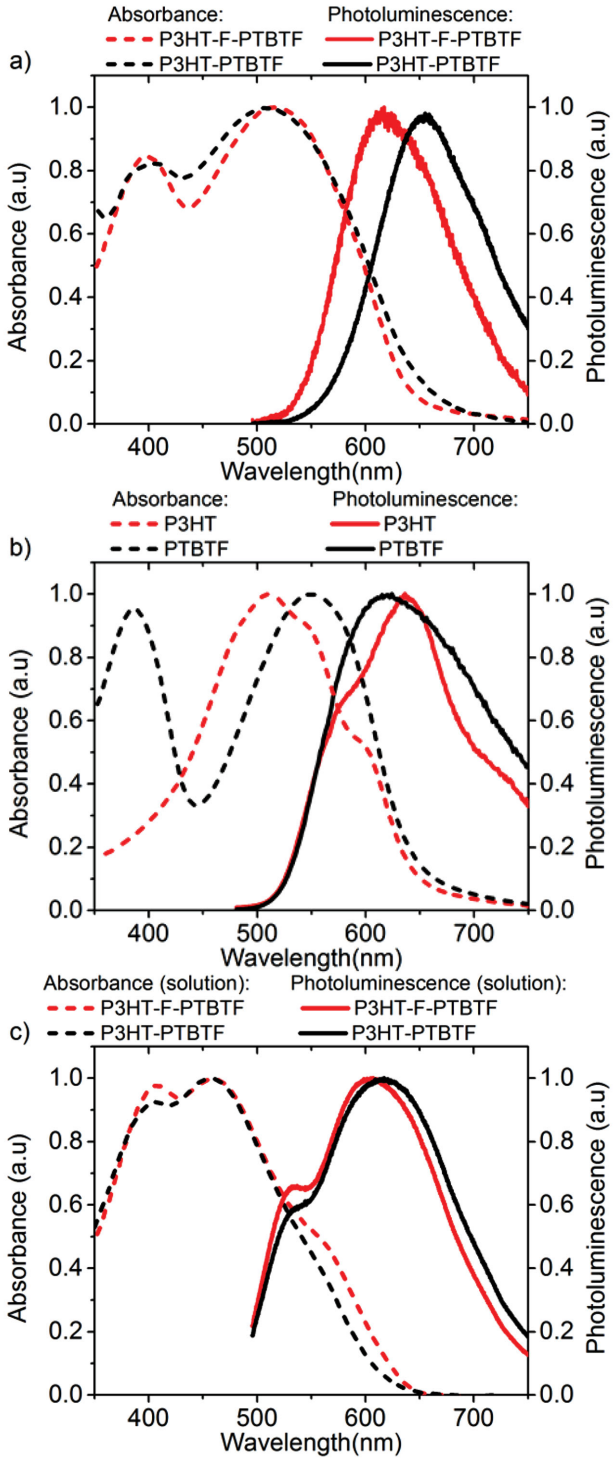

Figure 4. Steady-state absorption and PL spectra of a) block copolymer thin films, b) homopolymer thin films, and c) block copolymers in chloroform solution (0.01 mg mL^{-1}). Thin films were spin cast from chloroform (12 mg mL^{-1}) and further annealed at device conditions.

In the case of P3HT-PFTBT (Figure 5), in contrast to a broad PIA signal that is observed in P3HT-F-PTBTF or polymer blend OPVs,[21] positive differential transmission is observed from 600–700 nm at short times (0.1–10 ps). This corresponds to

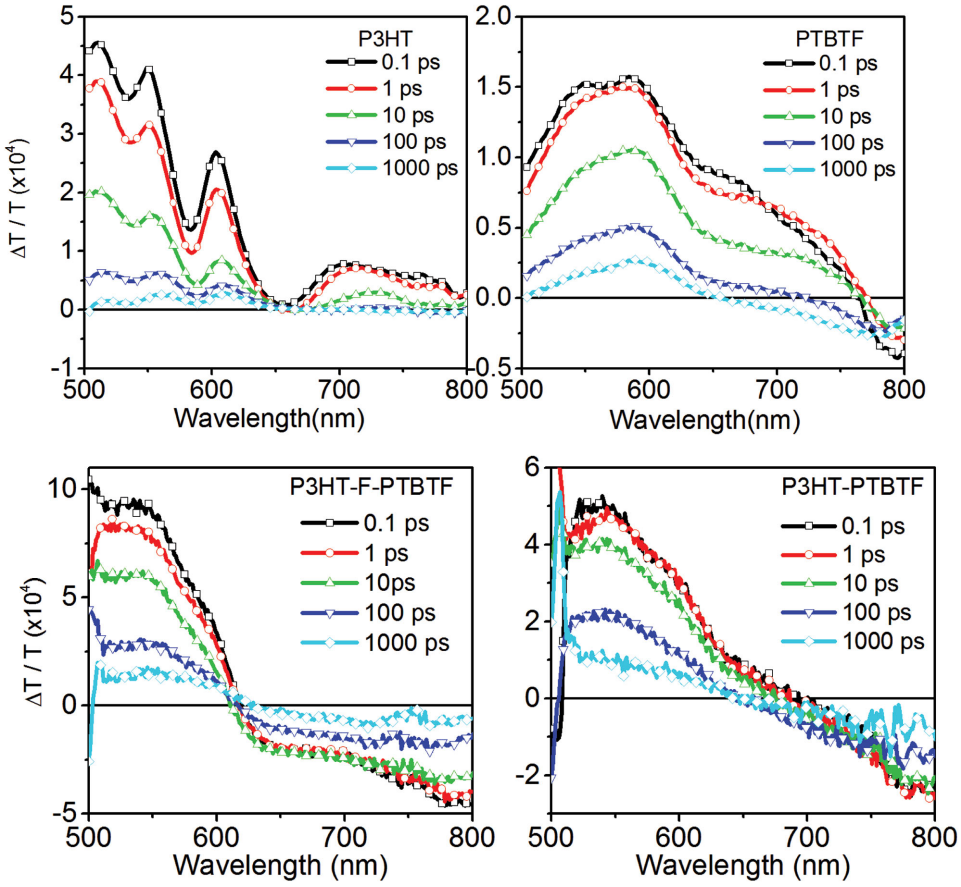

Figure 5. TA measurements of top) homopolymer and bottom) block copolymer films excited at 500 nm. Films were annealed at device conditions.

stimulated emission in these samples in the range matching the redshifted PL observed in P3HT-PFTBT films (Figure 4a). Stimulated emission is predominant at short times, and at longer times (>100 ps), the stimulated emission decays to reveal a weak PIA signal. This indicates that charge separation is significantly suppressed in P3HT-PTBTF compared with P3HT-F-PTBTF and other polymer photovoltaic blends.[13,25] This result is consistent with the device measurements and shows that the chemistry of the linking group influences the formation of photogenerated free charges.

The stimulated emission observed near 675 nm for P3HT-PTBTF corresponds to the PL maximum for P3HT-PTBTF (Figure 4a). Thus, we infer that the linking chemistry in P3HT-PTBTF results in the formation of a low-energy charge transfer state that does not decay to produce free charges. By contrast, in the case of P3HT-F-PTBTF, this low-energy charge transfer state is absent and charge separation occurs. This hypothesis is consistent with the device measurements, absorbance and PL characteristics, and transient absorption measurements. We also note that transient absorption measurements for both block copolymers in solution appear virtually identical, as shown in Figure S9 in the Supporting Information. P3HT is disordered in dilute solution and exhibits poor electronic properties, and as a result no evidence for charge separation is observed in either material.

Further insight into the kinetics for charge separation and recombination is gained by analyzing the time-dependent TA signals. Prior work has revealed two time scales for charge separation in polymer–fullerene and polymer–polymer blends.[25,27–30] The first timescale is ultrafast, occurs on <0.1 ps timescales, and corresponds to excitons generated near the donor–acceptor interface. A second, slower process is observed at longer times and is associated with excitons that must diffuse to the donor–acceptor interface before charge separation. The decay in the PIA signal is attributed to charge recombination. In polymer–polymer blends, in contrast to typical rates for recombination in polymer–fullerene blends, subnanosecond charge recombination has been observed.[21]

Figure 6b shows the kinetics of the PIA signal at 650 nm for both block copolymers. Similar to polymer–fullerene and polymer–polymer blends, charge separation in the P3HT-F-PTBTF system occurs rapidly, within 0.1 ps, as evidenced by the presence of a PIA signal at 0.1 ps. The PIA signal grows with time up to approximately 10 ps, rapidly decays beyond 10 ps, and within 2 ns the PIA decays completely. The growth in the PIA signal before 10 ps reflects an increase in polarons (free charges) from charge separation of excitons following diffusion to the donor–acceptor interface, while the decay beyond 10 ps reflects charge recombination processes. Our measurements thus reveal subnanosecond recombination kinetics in P3HT-F-PTBTF all-conjugated block copolymers. The kinetics for recombination in P3HT-F-PTBTF are much faster than that observed in polymer–fullerene blends but are comparable with those of

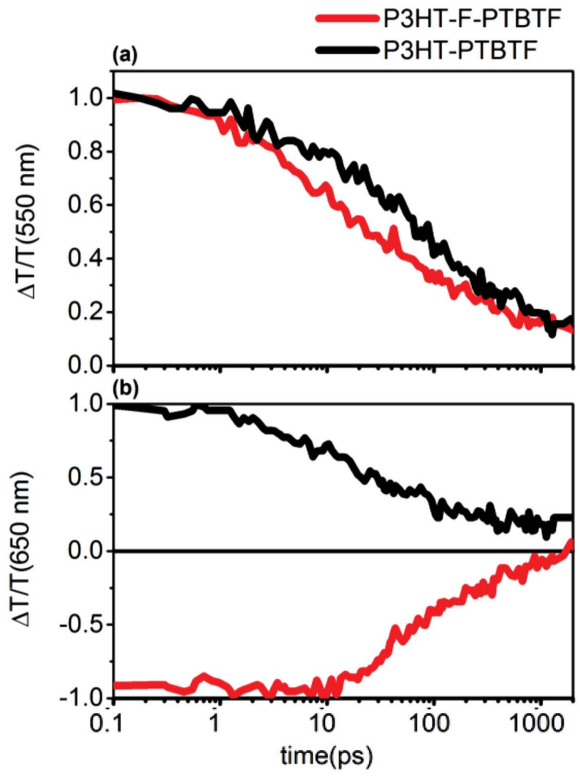

Figure 6. TA kinetics for block copolymer films annealed at 165 °C for 15 min, excited at 500 nm, and probed at a) 550 nm and b) 650 nm.

polymer–polymer blends.[21,25,27–29] While polymer–polymer blends were found to exhibit 30% loss of PIA intensity within 1 ns, here we observe almost 90% loss within 1 ns. Thus, losses through charge recombination are more significant in the present block copolymer systems compared with polymer–polymer and polymer–fullerene OPVs and may explain in part the relatively low efficiency of the best block copolymer systems (2–3%) compared with state-of-the-art polymer–polymer (4%–5%) and polymer–fullerene OPVs (7%–10%).[4,31–36]

Time constants for ground-state bleach (550 nm) and PIA (790 nm) were determined by a fit of the TA kinetics data using Equation (1)

$$\frac{\Delta T}{T} = A_1 \exp\left(\frac{t}{\tau_1}\right) + A_2 \exp\left(\frac{t}{\tau_2}\right) + A_3 \exp\left(\frac{t}{\tau_3}\right) \quad (1)$$

where normalized amplitudes A_i are given as percentages, and are shown in **Table 2**. Both systems show a fast initial decay, τ_1, with timescales comparable to P3HT/PCBM blends.[24]

Table 2. Decay parameters for block copolymers excited at 500 nm. Decay profiles were fit using Eq. 1.

	τ_1 [ps]	τ_2 [ps]	τ_3
P3HT-F-PTBTF (550 nm)	5 (41%)	60 (38%)	long (21%)
P3HT-PTBTF (550 nm)	2 (20%)	60 (51%)	long (29%)
P3HT-F-PTBTF (790 nm)	3 (17%)	30 (49%)	long (33%)
P3HT-PTBTF (790 nm)	2 (10%)	50 (39%)	long (51%)

However, the time constant τ_2 (≈30–60 ps) is much shorter compared to P3HT/PCBM blends.[37] This reflects rapid PIA decay kinetics, and suggests that further optimization of the linking group is needed to slow down charge recombination kinetics in conjugated block copolymer systems.

Molecular orbitals and electronic states at the block copolymer donor–acceptor interface were analyzed by density functional theory calculations to gain insight into the electronic properties of the donor–acceptor interface. Model oligomeric systems with 4 thiophene units and either TBT-F or F-TBT monomer were analyzed and are shown in **Figure 7**. For both P3HT-TBTF and P3HT-FTBT, HOMO levels reside on the TBTF unit while HOMO-1 levels reside on the P3HT. On the other hand, the symmetries of the LUMO and LUMO+1 levels are clearly different between model oligomers. For both oligomers, the LUMO resides primarily on the TBT unit, which is adjacent to P3HT in the P3HT-TBTF system. The LUMO+1 levels are centered around the F unit in the P3HT-F-TBT system, with delocalization across two thiophene repeat units on P3HT and the benzothiadiazole (B) monomer. In the case of P3HT-TBT-F, electron density is localized around the TBT-F unit with no electron density on the P3HT units. These calculations demonstrate that the orientation of the conjugated linking group influences electronic states, consistent with the experimental observations above, which show that the chemistry of the linking group impacts excited states at the donor–acceptor interface, charge separation and recombination rates, and photovoltaic performance.

3. Conclusion

In summary, we studied two nearly identical all-conjugated block copolymers, P3HT-F-PTBTF and P3HT-PTBTF, which differ primarily in the chemistry of the linking group between donor and acceptor polymer blocks. We hypothesized that the linking chemistry would have a minimal impact on morphology but a significant effect on photovoltaic device performance by influencing charge separation and recombination processes. Indeed, structural probes show no differences at the size-scale of molecular packing, crystallization, and nanoscale ordering. However, the power conversion efficiencies of all-conjugated block s devices based on these materials differed by a factor of 40. Steady-state PL measurements revealed the formation of a unique excited state in P3HT-PTBTF which we attributed to a low-energy charge transfer state at the P3HT-TBT donot-acceptor junction. Transient absorption measurements revealed ultrafast charge separation in P3HT-F-PTBTF, but charge separation was delayed and suppressed in P3HT-PTBTF due to the low-energy charge transfer state in this system. This provides conclusive evidence that the linking chemistry has a strong impact on charge separation and recombination processes in all-conjugated block copolymer systems.

These results demonstrate that covalently linking donor and acceptor polymers can be both beneficial and detrimental to photovoltaic performance. First, the covalent linkage precludes large-scale phase separation, commonly observed in polymer-blend photovoltaic systems.[38–42] Large-scale phase separation is detrimental to photovoltaic performance, and

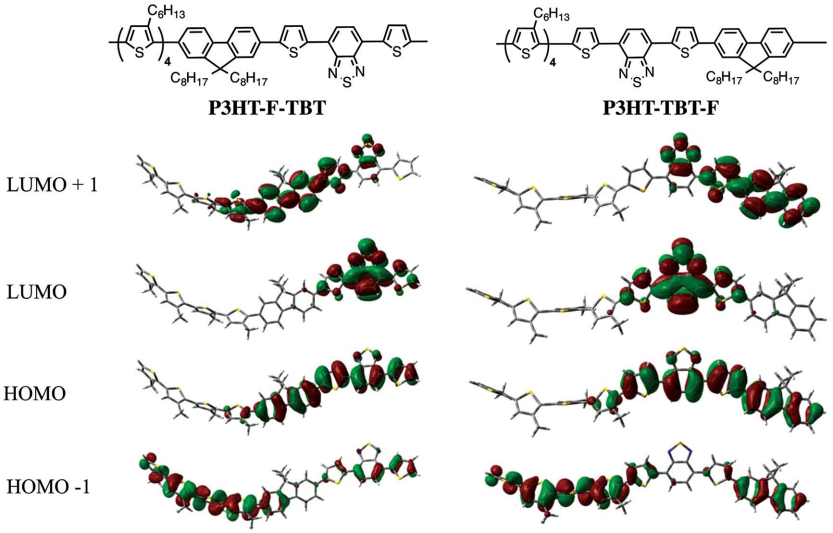

Figure 7. HOMO, LUMO, HOMO-1, and LUMO+1 levels in model P3HT-TBTF and P3HT-F-TBT oligomers.

therefore eliminating phase separation should improve photovoltaic performance. On the other hand, most block copolymer OPVs underperform relative to polymer–polymer blends. In this study, we demonstrate that improper design of the linking group can enhance charge recombination, resulting in very poor photovoltaic devices (<0.1% PCE). Furthermore, even for the optimal linking group chemistry studied in this report, our measurements indicate faster charge recombination compared with polymer–fullerene and polymer–polymer bulk heterojunction systems. Kinetic analysis indicates that even in P3HT-F-PTBTF, charge recombination occurs within 1 ns.

Thus, covalently linking donor and acceptor polymers can be detrimental to performance in at least two ways: through the formation of charge transfer states that do not produce free charges and through significantly increasing the rate for charge recombination. In order to address this and improve the photovoltaic performance of block copolymer OPVs, electronic coupling between donor and acceptor polymers should be decreased. Prior studies with donor–acceptor dyads and with polymer–polymer blend systems suggest that this can be accomplished by, for example, increasing the separation between donor and acceptor blocks.[6,41]

Finally, this work indicates that all-conjugated block copolymers may serve as useful model systems for the donor–acceptor interface in OPVs. Describing the progression from photoexcited states to free charges in OPV systems is a fundamental challenge in the field, and the interfaces of bulk heterojunction donor–acceptor blends are difficult to characterize, control, and study systematically.[22,43] All-conjugated block copolymers offer the possibility for systematically changing the composition and structure of the donor–acceptor interface.

Supporting Information

Supporting Information is available from the Wiley Online Library or from the author.

Acknowledgements

J.W.M., Y.H.L., and R.V. acknowledge the support of the National Science Foundation CAREER award (DMR-1352099) and CBET-1264703. Y.L. and E.D.G. acknowledge support from the Office of Naval Research under Grant No. N000141410532. This work was supported in part by the U.S. Department of Energy, Office of Science, Office of Basic Energy Sciences in the Institute for Molecular Engineering at Argonne National Laboratory under Contract No. DE-AC02-06CH11357. Use of the Center for Nanoscale Materials was supported by the U.S. Department of Energy, Office of Science, Office of Basic Energy Sciences, under Contract No. DE-AC02-06CH11357. Research carried out in part at the Center for Functional Nanomaterials, Brookhaven National Laboratory, which is supported by the U.S. Department of Energy, Office of Basic Energy Sciences, under Contract No. DE-AC02-98CH10886. Use of the National Synchrotron Light Source, Brookhaven National Laboratory, was supported by the U.S. Department of Energy, Office of Science, Office of Basic Energy Sciences, under Contract No. DE-AC02-98CH10886. The work at Los Alamos National Laboratory (LANL) was supported by the U.S. Department of Energy, Office of Basic Energy Sciences, under Work Proposal 08SPCE973 (W.N. and A.D.M.) and by the LANL LDRD program XW11 (A.D.M). This work was performed, in part, at the Center for Integrated Nanotechnologies, an Office of Science User Facility operated for the U.S. Department of Energy (DOE) Office of Science. Los Alamos National Laboratory, an affirmative action equal opportunity employer, is operated by Los Alamos National Security, LLC, for the National Nuclear Security Administration of the U.S. Department of Energy under contract DE-AC52-06NA25396.

Received: June 26, 2015
Published online: August 10, 2015

[1] A. Yassar, L. Miozzo, R. Gironda, G. Horowitz, *Prog. Polym. Sci.* **2013**, *38*, 791.
[2] M. J. Robb, S.-Y. Ku, C. J. Hawker, *Adv. Mater.* **2013**, *25*, 5686.
[3] S. B. Darling, *Energy Environ. Sci.* **2009**, *2*, 1266.
[4] C. Guo, Y.-H. Lin, M. D. Witman, K. A. Smith, C. Wang, A. Hexemer, J. Strzalka, E. D. Gomez, R. Verduzco, *Nano Lett.* **2013**, *13*, 2957.
[5] S.-S. Sun, C. Zhang, A. Ledbetter, S. Choi, K. Seo, C. E. Bonner, M. Drees, N. S. Sariciftci, *Appl. Phys. Lett.* **2007**, *90*.
[6] J. W. Verhoeven, H. J. van Ramesdonk, M. M. Groeneveld, A. C. Benniston, A. Harriman, *Chem. Phys. Chem.* **2005**, *6*, 2251.
[7] D. M. Hinkens, Q. Chen, M. K. Siddiki, D. Gosztola, M. A. Tapsak, Q. Qiao, M. Jeffries-El, S. B. Darling, *Polymer* **2013**, *54*, 3510.
[8] K. Johnson, Y.-S. Huang, S. Huettner, M. Sommer, M. Brinkmann, R. Mulherin, D. Niedzialek, D. Beljonne, J. Clark, W. T. S. Huck, R. H. Friend, *J. Am. Chem. Soc.* **2013**, *135*, 5074.
[9] M. P. Nikiforov, B. Lai, W. Chen, S. Chen, R. D. Schaller, J. Strzalka, J. Maser, S. B. Darling, *Energy Environ. Sci.* **2013**, *6*, 1513.
[10] R. C. Mulherin, S. Jung, S. Huettner, K. Johnson, P. Kohn, M. Sommer, S. Allard, U. Scherf, N. C. Greenham, *Nano Lett.* **2011**, *11*, 4846.
[11] C. R. McNeill, A. Abrusci, J. Zaumseil, R. Wilson, M. J. McKiernan, J. H. Burroughes, J. J. M. Halls, N. C. Greenham, R. H. Friend, *Appl. Phys. Lett.* **2007**, *90*, 193506.
[12] D. Mori, H. Benten, H. Ohkita, S. Ito, K. Miyake, *ACS Appl. Mater. Interfaces* **2012**, *4*, 3325.

[13] Y.-H. Lin, K. A. Smith, C. N. Kempf, R. Verduzco, *Polym. Chem.* **2013**, *4*, 229.
[14] W. Ma, C. Yang, X. Gong, K. Lee, A. J. Heeger, *Adv. Funct. Mater.* **2005**, *15*, 1617.
[15] K. A. Smith, B. Stewart, K. G. Yager, J. Strzalka, R. Verduzco, *J. Polym. Sci. Part B Polym. Phys.* **2014**, *52*, 900.
[16] Y.-H. Lin, K. A. Smith, C. N. Kempf, R. Verduzco, *Polym. Chem.* **2012**, *4*, 229.
[17] D. E. Johnston, K. G. Yager, H. Hlaing, X. Lu, B. M. Ocko, C. T. Black, *ACS Nano* **2013**, *8*, 243.
[18] K. A. Page, A. Kusoglu, C. M. Stafford, S. Kim, R. J. Kline, A. Z. Weber, *Nano Lett.* **2014**, *14*, 2299.
[19] W. Chen, M. P. Nikiforov, S. B. Darling, *Energy Environ. Sci.* **2012**, *5*, 8045.
[20] Y.-H. Lin, S. B. Darling, M. P. Nikiforov, J. Strzalka, R. Verduzco, *Macromolecules* **2012**, *45*, 6571.
[21] J. M. Hodgkiss, A. R. Campbell, R. A. Marsh, A. Rao, S. Albert-Seifried, R. H. Friend, *Phys. Rev. Lett.* **2010**, *104*, 177701.
[22] T. M. Clarke, J. R. Durrant, *Chem. Rev.* **2010**, *110*, 6736.
[23] D. Herrmann, S. Niesar, C. Scharsich, A. Köhler, M. Stutzmann, E. Riedle, *J. Am. Chem. Soc.* **2011**, *133*, 18220.
[24] I.-W. Hwang, D. Moses, A. J. Heeger, *J Phys. Chem. C* **2008**, *112*, 4350.
[25] R. A. Marsh, J. M. Hodgkiss, S. Albert-Seifried, R. H. Friend, *Nano Lett.* **2010**, *10*, 923.
[26] J. R. Moore, S. Albert-Seifried, A. Rao, S. Massip, B. Watts, D. J. Morgan, R. H. Friend, C. R. McNeill, H. Sirringhaus, *Adv. Energy Mater.* **2011**, *1*, 230.
[27] C. J. Brabec, G. Zerza, G. Cerullo, S. De Silvestri, S. Luzzati, J. C. Hummelen, S. Sariciftci, *Chem. Phys. Lett.* **2001**, *340*, 232.
[28] L. W. Barbour, R. D. Pensack, M. Hegadorn, S. Arzhantsev, J. B. Asbury, *J. Phys. Chem. C* **2008**, *112*, 3926.
[29] J. Guo, H. Ohkita, H. Benten, S. Ito, *J. Am. Chem. Soc.* **2010**, *132*, 6154.
[30] F. Etzold, I. A. Howard, R. Mauer, M. Meister, T.-D. Kim, K.-S. Lee, N. S. Baek, F. Laquai, *J. Am. Chem. Soc.* **2011**, *133*, 9469.
[31] Y. Zhou, T. Kurosawa, W. Ma, Y. Guo, L. Fang, K. Vandewal, Y. Diao, C. Wang, Q. Yan, J. Reinspach, J. Mei, A. L. Appleton, G. I. Koleilat, Y. Gao, S. C. B. Mannsfeld, A. Salleo, H. Ade, D. Zhao, Z. Bao, *Adv. Mater.* **2014**, *26*, 3767.
[32] H. Kang, K.-H. Kim, J. Choi, C. Lee, B. J. Kim, *ACS Macro Lett.* **2014**, *3*, 1009.
[33] H. Kang, M. A. Uddin, C. Lee, K.-H. Kim, T. L. Nguyen, W. Lee, Y. Li, C. Wang, H. Y. Woo, B. J. Kim, *J. Am. Chem. Soc.* **2015**, *137*, 2359.
[34] Y. Liang, Z. Xu, J. Xia, S.-T. Tsai, Y. Wu, G. Li, C. Ray, L. Yu, *Adv. Mater.* **2010**, *22*, E135.
[35] W. Li, L. Yang, J. R. Tumbleston, L. Yan, H. Ade, W. You, *Adv. Mater.* **2014**, *26*, 4456.
[36] Z. He, C. Zhong, S. Su, M. Xu, H. Wu, Y. Cao, *Nature Photon* **2012**, *6*, 591.
[37] T. Xiao, H. Xu, G. Grancini, J. Mai, A. Petrozza, U. S. Jeng, Y. Wang, X. Xin, Y. Lu, N. S. Choon, H. Xiao, B. S. Ong, X. Lu, N. Zhao, *Sci. Rep.* **2014**, *4*, 5211.
[38] J.-S. Kim, P. K. H. Ho, C. E. Murphy, R. H. Friend, *Macromolecules* **2004**, *37*, 2861.
[39] A. C. Arias, J. D. MacKenzie, R. Stevenson, J. J. M. Halls, M. Inbasekaran, E. P. Woo, D. Richards, R. H. Friend, *Macromolecules* **2001**, *34*, 6005.
[40] S. Westenhoff, I. A. Howard, R. H. Friend, *Phys. Rev. Lett.* **2008**, *101*, 016102.
[41] C. R. McNeill, S. Westenhoff, C. Groves, R. H. Friend, N. C. Greenham, *J. Phys. Chem. C* **2007**, *111*, 19153.
[42] C. R. McNeill, N. C. Greenham, *Adv. Mater.* **2009**, *21*, 3840.
[43] P. K. Nayak, K. L. Narasimhan, D. Cahen, *J. Phys. Chem. Lett.* **2013**, *4*, 1707.